Integrated analysis of circulating and tissue proteomes reveal fibronectin 1 is a potential biomarker in papillary thyroid cancer

Xu Qian (Qian_michelle2014@163.com)
Cancer Hospital of the University of Chinese Academy of Sciences, Zhejiang Cancer Hospital), Chinese Academy of Sciences

Guochao Ye
Huzhou Central Hospital

Xiaomei Zhang
Beijing Institute of Lifeomics

Mansheng Li
Beijing Institute of Lifeomics

Yongcan Xu
Huzhou Central Hospital

Haoru Dong
Cancer Hospital of the University of Chinese Academy of Sciences, Zhejiang Cancer Hospital), Chinese Academy of Sciences

Sheng Wang
Cancer Hospital of the University of Chinese Academy of Sciences, Zhejiang Cancer Hospital), Chinese Academy of Sciences

Yunping Zhu
Beijing Institute of Lifeomics

Xiaobo Yu
Beijing Institute of Lifeomics

Research Article

Keywords: Thyroid cancer proteome, Thyroid nodules, Indeterminate thyroid biopsy, Cancer secrotome, FN1

Posted Date: April 12th, 2022

DOI: https://doi.org/10.21203/rs.3.rs-1506256/v1

Additional Declarations: No competing interests reported.

Version of Record: A version of this preprint was published at BMC Cancer on May 8th, 2023. See the published version at https://doi.org/10.1186/s12885-023-10839-w.

Abstract

As the most frequent subtype of thyroid cancer, papillary thyroid cancer (PTC) has 20% indeterminate cases from preoperative cytology that could not be accurately diagnosed, which might lead to the surgical removal of the thyroid gland. To address this concern, we executed an in-depth analysis of serum proteomes of 26 PTC patients and 26 healthy controls using antibody microarrays and Data Independent Acquisition Mass Spectrometry (DIA-MS). The results identified a total of 1,091 serum proteins spanning 10–12 orders of magnitude, in which 157 differentially expressed proteins were identified that participate complement activation and coagulation cascades, platelet degranulation pathways. Furthermore, the analysis of serum proteomes before and after surgery indicate that the expression of proteins such as lactate dehydrogenase A, OR52B4 were changed which participate into fibrin clot formation and ECM-receptor interaction pathways. The further analysis of proteomes of PTC and neighboring tissues reveals integrin-mediated pathways that may cross talk between tissue and circulating compartment. Among these cross-talk proteins, circulating fibronectin 1 (FN1), gelsolin (GSN) and UDP-glucose 4-epimerase (GALE) were indicated as promising biomarkers to the PTC identification and validated in an independent cohort. To differentiate patients with benign nodule and PTC, the best ELISA result was from FN1 (sensitivity = 96.89%; specificity = 91.67%) which was tested in an independent cohort. Altogether, our results provide proteomic landscapes of PTC cancer before and after surgery as well as the cross-talk between tissue and circulating system, which would be valuable to understand the PTC pathology and improve PTC diagnostics in future.

Background

Thyroid cancer is the ninth most common malignancy worldwide [1]. In China, continuous increases of thyroid cancer were reported, i.e., the incidence rate increased from $2.75/10^5$ in 2000 to $19.42/10^5$ in 2012 in Zhejiang Province of China [2, 3]. Papillary thyroid cancer (PTC) is the most prevalent form of thyroid cancer and contributes mainly to the rapid increase of thyroid cancer [2, 4]. Over-surveillance and over-diagnosis of smaller differentiated cancers are considered to attribute to the increased epidemic and consequently, accompanied with overtreatment [5]. In this regard, efforts are urgently needed to prevent overtreatment of the low-risk papillary thyroid cancers with the aim to improve the quality of life and reduce the economic burden [5, 6]. Notably, there are limitations of preoperative cytology by fine-needle aspiration (FNA) biopsy where 20% indeterminate cases are diagnosed [7]. Moreover, the majority of the indeterminate cases is found to be benign nodules on histopathology after surgery [7]. There are potential risks and side-effects associated with overtreatment such as hypoparathyroidism, the lifelong thyroid hormone (levothyroxine) replacement therapy after total thyroidectomy, etc. Therefore, there is unmet need to identify which thyroid nodules are benign and unnecessary go to the FNA or surgery.

The molecular testing such as *BRAF V600E* mutations is suggested to distinguish aggressive PTCs that *BRAF V600E* mutation accounts for 60% of mutations in thyroid cancer [8]. Recent studies have shown that combination of BRAF V600E mutation and the Bethesda System for Reporting Thyroid Cytopathology system had increased sensitivity (89.57%) for malignant nodules and negative predictive

value (45.45%) for benign nodules in patients underwent ultrasound-guided FNA [9]. However, these genotyping of PTCs have not been established in routine practice and need further longitude large cohort study.

We hypothesized that incorporation of tumor-specific functional proteomic markers in the circulation holds promise to help determine a suspicious nodule. Previously, proteomics-based approaches have been successfully identified subtypes of certain cancers including gastric cancer, hepatocellular carcinoma and lung adenocarcinoma [10–12]. Studies in PTC tissues or FNA samples have demonstrated a spectrum of proteins or metabolics in the thyroid tissues has the potential to differentiate malignant thyroid nodules [13, 14]. While these candidate tissue biomarkers warrant further clinical validation, developing a minimally invasive test that is blood-based biomarker discovery for early diagnosis of PTC and treatment monitoring would also be important. Ideally, secretomes may reflect the status of diseased and healthy cells temporally. To test this hypothesis, we used an in-depth serum proteomics platform including customizable antibody microarrays and Data Independent Acquisition Mass Spectrometry (DIA-MS) to detect the differential serum protein expression by measuring paired serum, tumor tissues and their paired non-cancerous adjacent tissues (NATs) for the same patient with PTC [15]. This platform enables us to detect low-abundance proteins by spanning 10 orders of magnitude in protein concentration. We demonstrate a crosstalk of serum and tissue proteome and provide new insights into the oncobiology of PTC. We conclude from these findings that these relatively noninvasive candidate circulating proteins, which could be performed with frequency, may aide the clinical decision-making process and warrant further clinical validation for predicting malignancy.

Methods

Clinical samples and patient characteristics

Fresh frozen cancer tissues, paired NATs and serum samples before and after thyroidectomy were obtained from 26 patients with PTC. Serums from 26 healthy controls (NCs) were also obtained. The patients and NCs participating in this study all signed an institutional review board-approved informed consent form. This study was approved by the local Ethics Committee of Zhejiang Cancer Hospital (#IRB-2020-371) and Huzhou Central Hospital (#IRB-20180804-01). The patients and NCs were similar in age with a mean age of 39.7 ± 12.8. The 8th edition of tumor/lymph node/metastasis (TNM) staging system of the American Joint Committee on Cancer was used to define the stage of all patients. Most of PTC patients were staged as stage I (25of 26) and TI-RADS Score 6 (25 of 26) (Table 1). $BRAF^{V600E}$ mutation was found in 13 patients. Our validation cohort includes serum samples from 36 patients with benign nodules and 61 patients with PTC (data not shown).

Table 1
Clinicopathological characteristics of patients with papillary thyroid cancer (n = 26).

Variables	N	%
Age, y, mean ± SD (range)	26	39.7 ± 12.8
Sex		
Male	7	26.9
Female	19	73.1
T stage		
T1/T2	21	80.8
T3/T4	5	19.2
LNM		
N0	14	53.8
N1	12	46.2
TNM stage		
I	25	96.2
III	1	3.8
TI-RADS Score		
4	1	3.8
6	25	96.2
$BRAF^{V600E}$		
Mutant	13	50.0
Wild	2	7.7
Unknown	11	42.3

Screening of serum proteome using antibody microarrays

The antibody microarrays were prepared as previously described [15]. 10 μL of serum was diluted 1:10 with phosphate buffered saline (PBS; pH 7.4) and then labeled by NHS-PEG4-Biotin (Thermo Fisher Scientific, MA, USA). After removing the excess biotin molecules, the biotinylated serum was diluted with 400 μL of 5% milk (w/v) and then incubated with antibody microarrays that have been blocked for 1 h at room temperature with 500 μL of 5% milk (w/v). Subsequently, the antibody microarrays were washed

with PBS containing 0.05% (w/v) Tween 20 (PBST). The bound proteins on microarrays were detected by incubating with 2 μg/mL streptavidin-Phycoerythrin (PE) (Jackson Immunoresearch, USA) for 1 h at room temperature. After washing and drying, the microarrays were scanned using the GenePix 4300A microarray scanner.

Measurement of serum and tissue proteome using DIA-MS

Protein separation, peptide sample preparation and data-independent acquisition (DIA) analysis were performed as previously described [16]. Briefly, total protein was extracted from tumor tissues and their paired non-cancerous adjacent tissues (NATs) using RIPA buffer containing 10% protease inhibitor cocktail. The protein concentration was quantified by the Bradford method. The serum samples were diluted with lysis buffer containing 6 M urea (Sigma, USA). Next, extracted tissue protein and diluted serum were reduced with 10 mM Dithiothreitol (DTT) at 37℃ for 60 min. After alkylating with 500 mM Iodoacetamide (IAA) at room temperature for 45 min in dark, the protein was digested with trypsin. The concentrations of tryptic peptides determined by absorbance measurements with NanoDrop spectrophotometers (Thermo Scientific, USA). For construction of spectral library, 10 μg of peptides pool from each sample were separated into 10 fractions and Data Dependent Acquisition (DDA) analysis was performed on QE-HF mass spectrometer (Q Exactive HF Hybrid Quadrupole OrbitrapTM, Thermo Fisher). A human subset of the UniProt proteins FASTA database was used to generate spectral library using Spectronaut Pulsar X 12.0 (Biognosys, Schlieren, Switzerland) with the BGS factory setting. For DIA analysis, 1.5 μg peptides were separated on a 30 min LC gradient using an analytical column (150 μm × 250 mm, 2 μm 200 Å C18 particles) and analyzed by the mass spectrometry described above. The DIA acquisition scheme consisted of 45 fixed Windows ranging from 350 to 1500 m/z. The resolution distribution of MS1 and MS2 is 60000 and 30000, respectively. For quantification, DIA data were input into Spectronaut with peptides FDR and Proteins FDR setting at 1% and the iRT Local (Non-Linear) regression.

RNA-seq analysis

Gene count data (RNA-seq) of thyroid carcinoma samples were downloaded from The Cancer Genome Atlas database (TCGA; https://portal.gdc.cancer.gov/repository). The annotation information was downloaded from GENCODE (GRCh38.p13) catalog (https://www.gencodegenes.org/). Averaged values were taken for multiple probes sharing a same gene simple. Next, “edgeR” package was utilized to perform differential expression analysis (adjusted P value < 0.05 and |fold change (FC)| > 1). The quantified data were standardized with “scale” function in R. The heatmap was performed by using “pheatmap” package. 29 differentially expressed genes, consistent with the results of proteomic analysis, were shown in the heatmap. Gene ontology (GO) and Kyoto Encyclopedia of Genes and Genomes (KEGG) were conducted by “clusterProfiler”, “org.Hs.eg.db”, “enrichplot” packages in R to provide functional annotation and analyze pathway enrichment analyses. Adj.P < 0.05 was considered of statistical significance. GO enrichment analysis contains Molecular Function (MF), Biological Process (BP), Cellular Component (CC). The top 15 of KEGG pathways and top 5 of each GO terms were visualized by “GOplot” package.

Validation of biomarker candidates by IHC and ELISA

After deparaffinization in xylene, hydration with graded alcohol, and antigen retrieval, the tissue sections were placed in 3% hydrogen peroxide (H_2O_2) for 10 min at room temperature to inactivate endogenous peroxidases. The slides were washed three times in phosphate buffer saline(PBS), blocked with 2% bovine serum albumin (BSA) for 30 min at room temperature and incubated with primary antibodies at 4°C overnight. On the second day, after washing with PBS, the slides were incubated with HRP-conjugated secondary antibodies for 60 min at 37°C. The slides were then washed in PBS, followed by detection with DAB staining solution and counterstaining with hematoxylin.

The levels of Gelsolin and Fibronectin in the serum of the different treatment groups were measured by their respective ELISA kits. The optical density of each sample was measured at 450 nm using a Spectra Max 190 microplate reader.

Statistical and bioinformatics analysis

For the Antibody-array data, the intensities of identified proteins were corrected by subtracting background signal, then the values were log2 transformed and inter-array normalized with a quantile normalization followed by a mean centered. After background correction and signal normalization, the intensities can be used for the downstream analysis. For the MS data, the quantification values of identified proteins were log2 transformed and mean normalized.

To test for significant differences in the expression of proteins between samples from healthy and PTC patients before and after thyroidectomy, multiple comparisons were performed with the R package Limma (V3.38.3) [17]. Then, to determine the proteins that displayed significant differences in expression between each two groups, all pairwise comparisons of the three experimental groups were performed using Limma as well. Hits with P value < 0.05 were considered statistically significant. To identify Tumor versus NAT differential proteins, a modified t-test implemented in Limma was applied to tissue proteomic data. Proteins with P value < 0.05 were considered to be tumor-associated proteins.

Volcano plot, as well as the heatmap of significant proteins were performed using R package ggplot2 and ComplexHeatmap (distance: Pearson, linkage: complete) [18]. The distribution of serological protein concentrations detected by our DIA-MS and microarray platform using the reference concentrations from the human plasma proteome database (http://www.plasmaproteomedatabase.org/). The online tool DAVID (https://david.ncifcrf.gov/) was used to annotate proteins according to biological processes, cellular components, and molecular functions within the GO and KEGG pathway analyses [19]. Protein interactome network was built using Cytoscape (version 3.7.1) [20] and the protein-protein interactions were retrieved from the STRING database [21]. The common differentially expressed proteins from serum and tissue proceeded to in-depth analysis based on the Ingenuity Pathway Analysis (IPA).

The area under a receiver operating characteristic (ROC) curve and graphs of the true positive rate (sensitivity) and the false positive rate (1-specificity) were used to determine the diagnosis accuracy the

ELISA test.

Results

Serum proteomic analysis shows dysregulation in multiple biological processes in PTC patients

We characterized a total of 1091 serum proteins with an overlap of 159 proteins as detected through customizable antibody microarrays and DIA-MS (Fig. 1). Quality control demonstrates that the *r* correlations for array-to-array and slide-to-slide were 0.70 and 0.94 for antibody microarrays, respectively (Supplementary Fig. 1). The Pearson correlation analysis demonstrates a clearly grouping of proteins among all samples acquired by DIA-MS (Fig. 1, Supplementary Fig. 1). Proteins acquired from antibody microarrays and DIA-MS are belonged to the same cellular components (Fig. 1). In particular, a spectrum of proteins was associated with signaling pathways such as integrin signaling pathways, angiogenesis, blood coagulation, glycolysis, inflammation mediated pathway, interleukin and CCKR-pathway (Fig. 1).

We first sought to define the serum proteomic of PTC patients and the controls. We found 157 significantly differential expressed proteins between each group (adjusted p-value < 0.05) (Fig. 2). These dysregulated proteins mainly belong to the complement and coagulation cascades, platelet degranulation pathways (Fig. 2). In addition, PTC patients had activated pathways including extracellular matrix (ECM)-receptor interaction, proteoglycans, cell adhesion molecules and focal adhesion while the high-affinity immunoglobulin E receptor (FcεRI)- mediated signaling pathways were downregulated compared to normal controls (Fig. 2). Notably, an increased serum C3 and deceased serum apolipoprotein A4 in PTC patients are shown in our study and others by Mass Spectrometry and enzyme-linked immunosorbent assay (ELISA) validation [22].

We further analyzed the data to identify the association between proteomic changes and clinical data (Fig. 3). Pearson correlation analysis demonstrates APBA3 is positively correlated with serum levels of thyroglobulin (Tg) and negatively correlated with serum levels of Tg antibodies (TgAb). Tg is a iodoglycoprotein made by thyroid cells and serves as precursor for triiodothyronine (T3) and thyroxine (T4) hormones. Although serum levels of Tg cannot predict disease stage for PTC, the small thyroid remnants can be detected by serum levels of Tg during the follow-up after total thyroidectomy [23]. However, following lobectomy of patients with thyroid cancer, Tg level is inferenced by the lobe size, TSH levels, lymphocytic thyroiditis, thyroid nodules and other factors. It is challenged to detect Tg level produced by persistent/recurrent cancer tissue when the whole amount of Tg produced by the remaining lobe is measures. Thus, there is an unmet need for identifying other indicators for persistent cancer tissue and disease recurrence regard to the Tg dynamics. APBA3 is activator of hypoxia inducible factor 1 (HIF-1) and can mediate metastasis niche formation by recruiting monocytes and E-selectin induction in endothelial cells [24]. Its correlation with Tg and the underlying mechanism in thyroid cancer warrants further investigation.

There is substantial interest in the potential of proteomic profiling to aide risk stratification after surgery and to optimize the treatment decisions. We identified additional 58 significantly differential expressed serum proteins between PTC patients before and after tumor removal (Fig. 4). We found dysregulation of complement and coagulation cascades are main pathways between the two states. Intrinsic pathway of fibrin clot formation and intrinsic prothrombin activation pathway were activated in primary PTC patients without treatment and pathways like intrinsic pathway of fibrin clot formation and ECM-receptor interaction were downregulated after tumor removal. Notably, the serum level of lactate dehydrogenase A (LDHA) was decreased after tumor removal. This may reflect the change of tumor burden as seen in pervious study that LDHA is overexpressed in PTC tissue and represent an aggressive PTC behavior [25]. LDHA functions as an enzyme that convert pyruvate to lactate in the final step of glycolysis. These findings warrant further investigation in the follow-up of PTC patients in an independent cohort.

Proteomic features in PTC tumor tissues compared with NATs

We compared tumors vs paired NATs to identify PTC-associated alterations in proteins. 5648 total quantified proteins were identified and 4826 proteins were included in the final analysis after filtering with the missing value. Differential protein expression analysis results in 612 significantly dysregulated proteins between PTC tissues and NATs which accounts for 12.7% of the total quantified tissue proteome (Fig. 5). Among them, 344 were upregulated and 268 were downregulated in PTC tumor tissues. The represented proteins are shown in Fig. 5d. Notably, the number of proteins identified in the PTC tissues is significantly higher than that identified in the NATs. This finding is consistent to the common enriched pathways as seen in the functional pathway annotation and enrichment analysis of the dysregulated PTC proteomes which revealed that tissue-specific biological networks belong to protein translation and the immune system. Specifically, proteins involved in signal recognition particle (SRP)-dependent co-translational protein targeting to membrane, peptide chain elongation, MHC class II antigen presentation and metabolism-related pathways (Fig. 5). For example, the SRP is essential for delivering the proteome to the proper cellular membrane as integral membrane proteins or secretion [26].

We next compared the represented tumor-enriched proteins at a transcription level with TCGA data of PTC tumor and NAT transcriptomes (Fig. 6). The expression data of 568 thyroid carcinoma samples, including 510 tumor tissues and 58 NAT tissues, were downloaded from TCGA. After differential expression analysis, 2781 differentially expressed genes (DEGs) were screened and 29 DEGs, consistent with the results of proteomic analysis, were shown in the heatmap. The results of gene ontology (GO) biological processes and gene-set enrichment analysis with KEGG pathways showed 2781 DEGs were involved in such as neuroactive ligand-receptor interaction, cytokine-cytokine receptor interaction, complement and coagulation cascades, ECM-receptor interaction and organization, collagen-containing extracellular matrix and receptor ligand activity, tyrosine metabolism. Our analysis indicates similar clusters at the transcriptional level and protein level.

Integration of blood-thyroid proteome reveals an integrin-mediated signature in blood-tumor crosstalk

We analyzed the overlapping 23 proteins presented in both serum and thyroid tumor tissue proteomic dataset (Fig. 7). To gain insight into the biological pathways being related to molecular signals that may mediate blood-tumor tissue crosstalk, we used GO Term Finder to classify the pathways. We found that mitogen-activated protein kinase (MAPK) signaling for integrins and ECM proteoglycans were upregulated in PTC patients. Integrin is a family of transmembrane glycoprotein signaling receptors and its subunits can be found in platelets and tumor cells [27, 28]. Notably, the extracellular domain of integrin αvβ3 on the plasma membrane of tumor cells contain the receptor for thyroid hormone analogues [29]. It has been demonstrated that L-thyroxine (T4) bind the cell surface receptor on integrin αvβ3 and subsequently regulate cancer cell proliferation, angiogenesis and metastasis via MAPK (ERK1 and ERK2 cascade) pathway [29]. Additionally, BRAFV600E mutation is a risk factor for PTC being related to poor clinical outcome [30]. It has been demonstrated that BRAF mutation can activate MAPK pathway which is reversal by MAPK pathway inhibitors, for example, the mitogen-activated protein kinase inhibitor trametinib [31]. We have identified 13 of 26 patients harbored BRAFV600E mutation. In addition, platelet-tumor cell interaction has been proposed to participate in tumor metastasis [28]. Figure 8 demonstrate an IPA network of integrin-mediated pathways indicating the potential protein-protein interactions in PTC. It is interesting to further research on the T4 hormone-platelet/tumor cells via integrin singling in PTC model.

Serum fibronectin 1, gelsolin and UDP-glucose 4-epimerase have the potential to differentiate patients with benign nodules and PTC

Specifically, 23 overlapping proteins are significantly being correlated between PTC tissue and serum across patients. We observed higher expressions of fibronectin 1 (FN1), gelsolin (GSN) and UDP-glucose 4-epimerase (GALE) expression at the circulating and tissue level of PTC patients compared to controls acquired by antibody microarrays and DIA-MS. We also observed high expressions of FN1, GSN and GALE in PTC tissue compared to normal tissues by IHC (Figure S2B). The mRNA levels of FN1, GSN and GALE were also highly expressed in PTC tissues acquired by RNA-seq in TCGA dataset (Fig. 6). We further observed serum levels of FN1 and GSN were highly expressed in PTC patients compared to patients with benign nodules in an independent cohort by ELISA (Figure S2). The values of ELSIA tests were demonstrated in Table 2, FN1 (sensitivity = 96.89%; specificity = 91.67%), GSN (sensitivity = 83.33%; specificity = 50%), FN1 combined with GSN (sensitivity = 87.5%; specificity = 86.11%), respectively. FN1, a glycoprotein, is an important component of extracellular matrix. The biological role of FN1, especially FN1-beta1 integrin signaling for cancer progression and metastasis and therapy resistance has been explored in cancers such as lung cancer and breast cancer. GSN is a cytoskeletal protein that can promote epithelial-to-mesenchymal transition (EMT) signaling and subsequent tumor invasion. GALE is a

glycosyltransferase being involved in the galactose metabolism. It has been shown that mRNA level of GALE and FN1 were overexpressed in PTC compared to benign nodules acquired by RT-PCR [32]. These observations supported a potential role for serum FN1, GSN and GALE to differentiate patients with benign nodules and PTC. We did not validate the GALE and other proteins due to the lack of commercial ELISA kits. It is interesting for further validation of them as potential biomarkers independently or in a combination for PTC differential diagnostics in a large cohort.

Table 2
Area under the curve (AUC) and its 95% confidence interval (CI), sensitivity and specificity values of the ELISA tests.

	FN1	GSN	Combined
AUC (95% CI)	0.924 (0.867–0.98)	0.637 (0.493–0.78)	0.919 (0.850–0.988)
Sensitivity (%)	86.89	83.33	87.5
Specificity (%)	91.67	50	86.11

Discussion

Blood-based liquid biopsy has shown its advantages in clinical settings as a minimally invasive, safe, and alternative or complementary approach for tissue biopsies. Importantly, tumor derived secretomes or cancer degradomes in TME play central roles in tumor progression, recurrence and metastases [33]. While DNA or RNA sequence data have been utilized to guide cancer treatment, a recent study demonstrates that cancer proteome is complement to DNA/RNA status and has the potential to refine treatment options [34]. In addition, proteome-wide depiction of interactomes across cancer and host response at tissue and circulating level remains elusive. Here, we performed a comprehensive analysis of tissue and serum proteomes from PTC patients and healthy controls. We applied a strategy employing antibody microarrays and DIA-MS to quantify a total of 1091 serum proteins that results much improved depth of serum proteome. Integrative analyses reveal that integrin-mediated pathways are at the nexus of crosstalk between blood and tumor and complement activation and coagulation cascades at the circulating level may promote tumor growth. These findings improve our knowledge of thyroid cancer biology and hence potentially aide the clinical decision-making process.

We identified a dysregulation of integrin-mediated pathways underlying blood-tumor crosstalk in PTC patients. This finding adds to recent discussions on the roles of thyroid hormones (THs) on thyroid cancer proliferation, metastasis, angiogenesis, radio-resistance via the integrin which is overexpressed in cancer cells [35]. L-thyroxine (T4) receptor, not T3 receptor, on integrin αvβ3 has been recognized as a principle ligand of the thyroid hormone analogue receptor in cancer cells [36]. It has been demonstrated

that the bioactivity of T4 include promoting cancer cell proliferation, migration, angiogenesis and platelet interaction [37]. The underlying mechanism may be the activation of MAPK pathway that promotes papillary and follicular thyroid cancer cell proliferation in response to T4 and inhibition of p53-dependent apoptosis of tumor cells [38, 39]. We also show the dysregulation of MAPK signaling for integrin in PTC patients in our analysis. To be noted that, T4 concentrations of PTC patients are within the reference range in our study. This phenomenon has been shown in a previous study that T4 at physiological concentrations initiates at the iodothyronine receptor on cell surface integrin αvβ3 and activate cancer cell proliferation in vitro and in xenografts [35].

One other possible T4-related mechanism is the actions on the EMT process [40]. Our analysis based on proteomic data in PTC patients identified EMT markers FN1, GSN and GALE are strongly expressed in PTC tissues and also at the circulating level. We further show that higher expressions of FN1, GSN and GALE in PTC tissues compared to NATs. This finding is consistent to the transcriptional level of FN1, GSN and GALE expressions in TCGA dataset of thyroid cancer. In particular, integrin αvβ3 contains an Arg-Gly-Asp (RGD) recognition binding site specially for ECM proteins such as FN1 and thyroid hormones bind the receptor near the RGD site to that serves as a recognition and binding motif for ECM proteins [41, 42]. Previous study has been demonstrated that lncRNA *NEAT1* can modulate miR-491 levels to regulate transglutaminase 2 (TGM2) and promote the transcriptional activation of FN1 through nuclear factor kappa B (NFkb) p65 nuclear translocation and consequently, lead to the PTC invasion and metastasis [43]. In addition, overexpression of FN1 is also found in adioactivity iodine (RAI)- resistant PTC tissues where lncRNA-NEAT1/miR-101-3p/FN1 axis and PI3K/AKT signaling pathway are involved [44]. Importantly, downregulation of *NEAT1* can reverse the RAI resistance of PTC [44]. For GALE, its mRNA expression was also found being increased in PTC tissues, but its role in PTC remains to be explored [32]. Additionally, we have validated serum FN1 and GSN to differentiate patients with benign nodules and PTC by Elisa tests. The best ELISA result was from FN1 (sensitivity = 96.89%; specificity = 91.67%). Thus, we believe that additional studies are warranted to validate the serum levels of FN1, GSN and GALE as potential biomarkers for PTC in independent datasets from a large perspective clinical study.

In this study, we also demonstrate dysregulation of complement activation and coagulation cascades at the circulation level which are critical factors for cancer initiation or progression. The human complement system consists of about 50 serum proteins and membrane-bound regulators and receptors [45]. It has been widely demonstrated that imbalanced complement activation contribute to regulating the functions and tumor-suppressing immune responses [46]. Therapeutic targeting of complement system is also discussed [46].

In summary, the work presented here identifies a resource comprising proteomic regulations in the PTC tumor and circulation, highlights that integrin-mediated pathways, as well as complement activation and coagulation cascades, are regulated, and distinguishes FN1, GSN and GALE as promising biomarkers to achieve the diagnostics for those indeterminate cases. Notably, as discussed above, thyroid hormones can also regulate thyroid cancer cell proliferation through molecular and signaling pathways. The therapeutic targeting impinging on these signaling pathways thus best be explored. For example, the T4

analogue, tetraiodothyroacetic acid (tetrac) can block the actions of T4- integrin αvβ3 in thyroid cancer [35]. Besides, T3 signaling through thyroid hormone receptor beta (TRβ) in the nucleus has a tumor-suppressive effect [35]. In addition, thyroid hormone levels are regulated by the thyroid stimulating hormone (TSH) released from the pituitary. Sulaieva et al. show that TSH levels are not associated with PTC aggressiveness including LNM, TNM stage, and BRAFV600E mutation [47]. Given by the complex of thyroid hormone regulation, future studies should also address their ability in relation to thyroid cancer.

Abbreviations

AA: antibody microarrays; DIA: Data Independent Acquisition Mass Spectrometry; Array: antibody microarrays; TB: test before surgery of PTC patients; Norm: healthy individuals; TA: test after surgery of PTC patients; TP: paired non-cancerous adjacent tissues; TC: tumor tissues.

Declarations

Acknowledgements

Gene count data (RNA-seq) of thyroid carcinoma samples were downloaded from The Cancer Genome Atlas database (TCGA; https://portal.gdc.cancer.gov/repository). The annotation information was downloaded from GENCODE (GRCh38.p13) catalog (https://www.gencodegenes.org/).

Authors' contributions

X.Q contributed to conceiving the concept, lab management, supervision, funding acquisition, wrote the first draft of the manuscript. G.Y, X.Z, Y.X, S.W and H.D contributed to lab research, M.L and Y.Z contributed to data analysis. X.Q and X.Y revised the manuscript.

Funding

This work was supported by the Zhejiang Provincial Natural Science Foundation of China (LGF21H200002), the National Natural Science Foundation of China (81702091, 31870823), the Internal Talent Program (Under Forty) of Zhejiang Cancer Hospital, the National Key R&D Program of China (2020YFE0202200) and State Key Laboratory of Proteomics (SKLP-O202007).

Availability of data and materials

The datasets used and/or analysed during the current study are available from the corresponding author on reasonable request. Correspondence and requests for materials should be addressed to X.Q or X.Y. or Y.Z..

Declarations

Ethics approval and consent to participate

All the methods were performed in accordance with the Declaration of Helsinki guidelines and regulations. The retrospective serum and tissue samples were used for the study after approval from the local Ethics Committee of Zhejiang Cancer Hospital (#IRB-2020-371) and Huzhou Central Hospital (#IRB-20180804-01). The informed consent was obtained from all the subjects and/or legal guardians.

Consent for publication

Not applicable.

Competing interests

The authors declare that they have no competing interests.

References

1. Fitzmaurice C, Dicker D, Pain A, Hamavid H, Moradi-Lakeh M, MacIntyre MF, Allen C, Hansen G, Woodbrook R, Wolfe C*et al*: **The Global Burden of Cancer 2013**. *JAMA oncology*2015, **1**(4):505-527.
2. Du L, Wang Y, Sun X, Li H, Geng X, Ge M, Zhu Y: **Thyroid cancer: trends in incidence, mortality and clinical-pathological patterns in Zhejiang Province, Southeast China**. *BMC cancer*2018, **18**(1):291.
3. Xie SH, Chen J, Zhang B, Wang F, Li SS, Xie CH, Tse LA, Cheng JQ: **Time trends and age-period-cohort analyses on incidence rates of thyroid cancer in Shanghai and Hong Kong**. *BMC cancer*2014, **14**:975.
4. Ahn HS, Kim HJ, Kim KH, Lee YS, Han SJ, Kim Y, Ko MJ, Brito JP: **Thyroid Cancer Screening in South Korea Increases Detection of Papillary Cancers with No Impact on Other Subtypes or Thyroid Cancer Mortality**. *Thyroid : official journal of the American Thyroid Association*2016, **26**(11):1535-1540.
5. Davies L, Hoang JK: **Thyroid cancer in the USA: current trends and outstanding questions**. *The lancet Diabetes & endocrinology*2021, **9**(1):11-12.
6. Lamartina L, Grani G, Durante C, Filetti S, Cooper DS: **Screening for differentiated thyroid cancer in selected populations**. *The lancet Diabetes & endocrinology*2020, **8**(1):81-88.
7. Filetti S, Durante C, Hartl D, Leboulleux S, Locati LD, Newbold K, Papotti MG, Berruti A: **Thyroid cancer: ESMO Clinical Practice Guidelines for diagnosis, treatment and follow-up†**. *Annals of oncology : official journal of the European Society for Medical Oncology*2019, **30**(12):1856-1883.
8. Cancer Genome Atlas Research Network:**Integrated genomic characterization of papillary thyroid carcinoma**. *Cell*2014, **159**(3):676-690.
9. Sheng D, Yu X, Li H, Zhang M, Chen J: **BRAF V600E mutation and the Bethesda System for Reporting Thyroid Cytopathology of fine-needle aspiration biopsy for distinguishing benign from malignant thyroid nodules**. *Medicine*2021, **100**(37):e27167.
10. Ge S, Xia X, Ding C, Zhen B, Zhou Q, Feng J, Yuan J, Chen R, Li Y, Ge Z*et al*: **A proteomic landscape of diffuse-type gastric cancer**. *Nature communications*2018, **9**(1):1012.

11. Jiang Y, Sun A, Zhao Y, Ying W, Sun H, Yang X, Xing B, Sun W, Ren L, Hu B*et al*: **Proteomics identifies new therapeutic targets of early-stage hepatocellular carcinoma**. *Nature*2019, **567**(7747):257-261.
12. Xu JY, Zhang C, Wang X, Zhai L, Ma Y, Mao Y, Qian K, Sun C, Liu Z, Jiang S*et al*: **Integrative Proteomic Characterization of Human Lung Adenocarcinoma**. *Cell*2020, **182**(1):245-261.e217.
13. DeHoog RJ, Zhang J, Alore E, Lin JQ, Yu W, Woody S, Almendariz C, Lin M, Engelsman AF, Sidhu SB*et al*: **Preoperative metabolic classification of thyroid nodules using mass spectrometry imaging of fine-needle aspiration biopsies**. *Proc Natl Acad Sci U S A*2019, **116**(43):21401-21408.
14. Sun, Y., Selvarajan, S., Zang, Z., Liu, W., Zhu, P. Y., Zhang, H., Chen, H., Cai, X., Gao, H., Wu, Z., *et al*: **Protein classifier for thyroid nodules learned from rapidly acquired proteotypes**. *bioRxiv* 2020.
15. Xu M, Deng J, Xu K, Zhu T, Han L, Yan Y, Yao D, Deng H, Wang D, Sun Y*et al*: **In-depth serum proteomics reveals biomarkers of psoriasis severity and response to traditional Chinese medicine**. *Theranostics*2019, **9**(9):2475-2488.
16. Wang G, Wang Y, Zhang L, Cai Q, Lin Y, Lin L, Lin X: **Proteomics analysis reveals the effect of Aeromonas hydrophila sirtuin CobB on biological functions**. *J Proteomics*2020, **225**:103848.
17. Ritchie ME, Phipson B, Wu D, Hu Y, Law CW, Shi W, Smyth GK: **limma powers differential expression analyses for RNA-sequencing and microarray studies**. *Nucleic Acids Res*2015, **43**(7):e47.
18. Gu Z, Eils R, Schlesner M: **Complex heatmaps reveal patterns and correlations in multidimensional genomic data**. *Bioinformatics*2016, **32**(18):2847-2849.
19. Huang da W, Sherman BT, Lempicki RA: **Systematic and integrative analysis of large gene lists using DAVID bioinformatics resources**. *Nat Protoc*2009, **4**(1):44-57.
20. Shannon P, Markiel A, Ozier O, Baliga NS, Wang JT, Ramage D, Amin N, Schwikowski B, Ideker T: **Cytoscape: a software environment for integrated models of biomolecular interaction networks**. *Genome Res*2003, **13**(11):2498-2504.
21. Szklarczyk D, Gable AL, Nastou KC, Lyon D, Kirsch R, Pyysalo S, Doncheva NT, Legeay M, Fang T, Bork P*et al*: **The STRING database in 2021: customizable protein-protein networks, and functional characterization of user-uploaded gene/measurement sets**. *Nucleic Acids Res*2021, **49**(D1):D605-d612.
22. Farrokhi Yekta R, Arefi Oskouie A, Rezaei Tavirani M, Mohajeri-Tehrani MR, Soroush AR: **Decreased apolipoprotein A4 and increased complement component 3 as potential markers for papillary thyroid carcinoma: A proteomic study**. *Int J Biol Markers*2018, **33**(4):455-462.
23. Schlumberger M, Leboulleux S: **Current practice in patients with differentiated thyroid cancer**. *Nat Rev Endocrinol*2021, **17**(3):176-188.
24. Hara T, Nakaoka HJ, Hayashi T, Mimura K, Hoshino D, Inoue M, Nagamura F, Murakami Y, Seiki M, Sakamoto T: **Control of metastatic niche formation by targeting APBA3/Mint3 in inflammatory monocytes**. *Proc Natl Acad Sci U S A*2017, **114**(22):E4416-E4424.
25. Ban EJ, Kim D, Kim JK, Kang SW, Lee J, Jeong JJ, Nam KH, Chung WY, Kim K: **Lactate Dehydrogenase A as a Potential New Biomarker for Thyroid Cancer**. *Endocrinol Metab (Seoul)*2021, **36**(1):96-105.

26. Wild K, Juaire KD, Soni K, Shanmuganathan V, Hendricks A, Segnitz B, Beckmann R, Sinning I: **Reconstitution of the human SRP system and quantitative and systematic analysis of its ribosome interactions**. *Nucleic Acids Res*2019, **47**(6):3184-3196.
27. Huang J, Li X, Shi X, Zhu M, Wang J, Huang S, Huang X, Wang H, Li L, Deng H*et al*: **Platelet integrin αIIbβ3: signal transduction, regulation, and its therapeutic targeting**. *J Hematol Oncol*2019, **12**(1):26.
28. Lavergne M, Janus-Bell E, Schaff M, Gachet C, Mangin PH: **Platelet Integrins in Tumor Metastasis: Do They Represent a Therapeutic Target?** *Cancers (Basel)*2017, **9**(10).
29. Davis PJ, Mousa SA, Lin HY: **Nongenomic Actions of Thyroid Hormone: The Integrin Component**. *Physiol Rev*2021, **101**(1):319-352.
30. Wang F, Zhao S, Shen X, Zhu G, Liu R, Viola D, Elisei R, Puxeddu E, Fugazzola L, Colombo C*et al*: **BRAF V600E Confers Male Sex Disease-Specific Mortality Risk in Patients With Papillary Thyroid Cancer**. *J Clin Oncol*2018, **36**(27):2787-2795.
31. Borrelli N, Panebianco F, Condello V, Barletta JA, Kaya C, Yip L, Nikiforova MN, Nikiforov YE: **Characterization of Activating Mutations of the MEK1 Gene in Papillary Thyroid Carcinomas**. *Thyroid*2019, **29**(9):1279-1285.
32. da Silveira Mitteldorf CA, de Sousa-Canavez JM, Leite KR, Massumoto C, Camara-Lopes LH: **FN1, GALE, MET, and QPCT overexpression in papillary thyroid carcinoma: molecular analysis using frozen tissue and routine fine-needle aspiration biopsy samples**. *Diagn Cytopathol*2011, **39**(8):556-561.
33. Fan J, Ning B, Lyon CJ, Hu TY: **Circulating Peptidome and Tumor-Resident Proteolysis**. *Enzymes*2017, **42**:1-25.
34. Wahjudi LW, Bernhardt S, Abnaof K, Horak P, Kreutzfeldt S, Heining C, Borgoni S, Becki C, Berg D, Richter D*et al*: **Integrating proteomics into precision oncology**. *Int J Cancer*2021, **148**(6):1438-1451.
35. Mousa SA, Hercbergs A, Lin HY, Keating KA, Davis PJ: **Actions of Thyroid Hormones on Thyroid Cancers**. *Front Endocrinol (Lausanne)*2021, **12**:691736.
36. Desgrosellier JS, Cheresh DA: **Integrins in cancer: biological implications and therapeutic opportunities**. *Nat Rev Cancer*2010, **10**(1):9-22.
37. Davis PJ, Mousa SA, Schechter GP, Lin HY: **Platelet ATP, Thyroid Hormone Receptor on Integrin αvβ3 and Cancer Metastasis**. *Horm Cancer*2020, **11**(1):13-16.
38. Lin HY, Tang HY, Shih A, Keating T, Cao G, Davis PJ, Davis FB: **Thyroid hormone is a MAPK-dependent growth factor for thyroid cancer cells and is anti-apoptotic**. *Steroids*2007, **72**(2):180-187.
39. Liu YC, Yeh CT, Lin KH: **Molecular Functions of Thyroid Hormone Signaling in Regulation of Cancer Progression and Anti-Apoptosis**. *Int J Mol Sci*2019, **20**(20).
40. Mousa SA, Glinsky GV, Lin HY, Ashur-Fabian O, Hercbergs A, Keating KA, Davis PJ: **Contributions of Thyroid Hormone to Cancer Metastasis**. *Biomedicines*2018, **6**(3).
41. Plow EF, Haas TA, Zhang L, Loftus J, Smith JW: **Ligand binding to integrins**. *J Biol Chem*2000, **275**(29):21785-21788.

42. Lin HY, Cody V, Davis FB, Hercbergs AA, Luidens MK, Mousa SA, Davis PJ: **Identification and functions of the plasma membrane receptor for thyroid hormone analogues**. *Discov Med*2011, **11**(59):337-347.
43. Sun W, Qin Y, Wang Z, Dong W, He L, Zhang T, Zhang H: **The**. *Front Oncol*2021, **11**:610547.
44. Liu C, Feng Z, Chen T, Lv J, Liu P, Jia L, Zhu J, Chen F, Yang C, Deng Z: **Downregulation of NEAT1 reverses the radioactive iodine resistance of papillary thyroid carcinoma cell via miR-101-3p/FN1/PI3K-AKT signaling pathway**. *Cell Cycle*2019, **18**(2):167-203.
45. Ricklin D, Hajishengallis G, Yang K, Lambris JD: **Complement: a key system for immune surveillance and homeostasis**. *Nat Immunol*2010, **11**(9):785-797.
46. Malik A, Thanekar U, Amarachintha S, Mourya R, Nalluri S, Bondoc A, Shivakumar P: **"Complimenting the Complement": Mechanistic Insights and Opportunities for Therapeutics in Hepatocellular Carcinoma**. *Front Oncol*2020, **10**:627701.
47. Sulaieva O, Chernenko O, Chereshneva Y, Tsomartova D, Larin O: **Thyroid stimulating hormone levels and BRAFV600E mutation contribute to pathophysiology of papillary thyroid carcinoma: Relation to outcomes?** *Pathophysiology*2019, **26**(2):129-135.

Figures

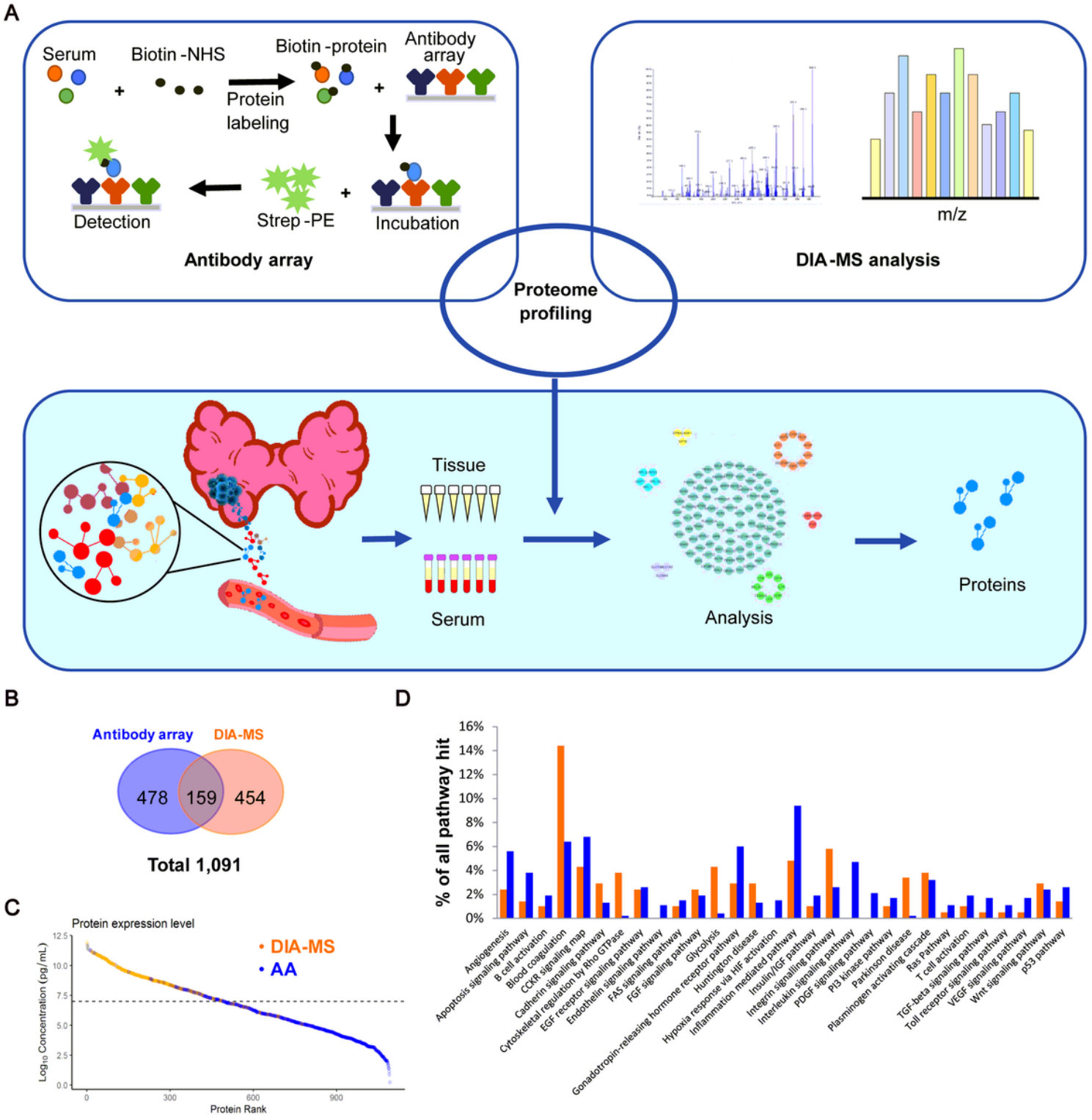

Figure 1

Study design using in-depth serum proteomics and tissue proteomics of papillary thyroid cancer (PTC). (A) work flow. (B) a total of 1091 serum proteins with an overlap of 159 proteins was detected through customizable antibody microarrays and DIA-MS. (C) Distribution of serum proteins detected by DIA-MS and antibody array two-pronged approach. (D) Proteins acquired from antibody microarrays and DIA-MS are belonged to the same cellular components.

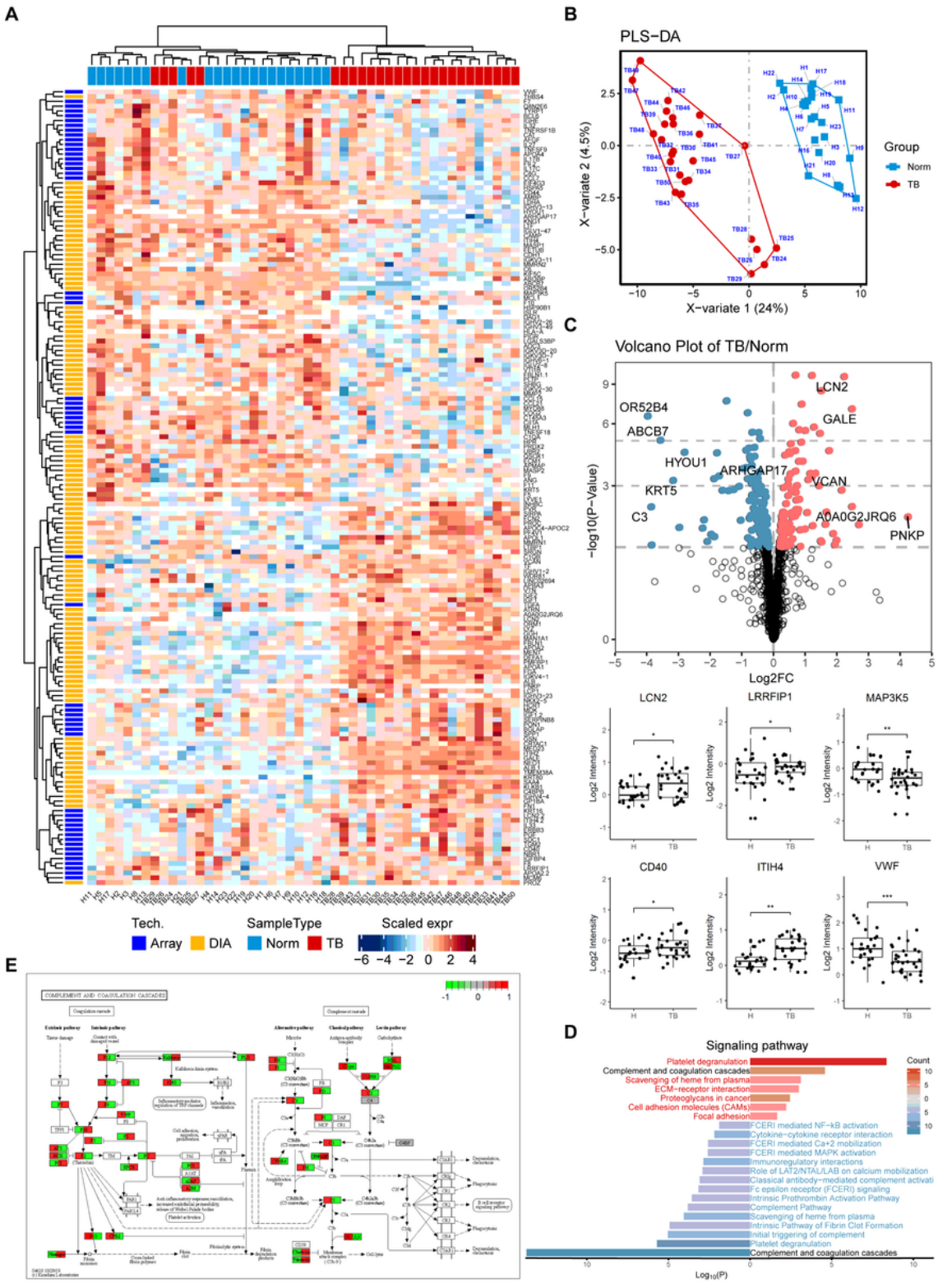

Figure 2

Serum proteome detection consisting of healthy individuals and patients with papillary thyroid cancer (PTC). (A) Classification of healthy and PTC patient groups based on differentially expressed proteins and unbiased clustering analysis. (B) Scores plot for Partial least square-discriminant analysis (PLS-DA). Score plot shows TB in red and controls in blue polygon. (C) Identification of PTC-associated proteins in serum using volcano plot analysis. Box plot analy-sis of represented PTC-associated serum proteins. (D)

are the comparison of protein classes and signaling pathways for PTC-associated proteins and healthy controls. E, the complement cascade.

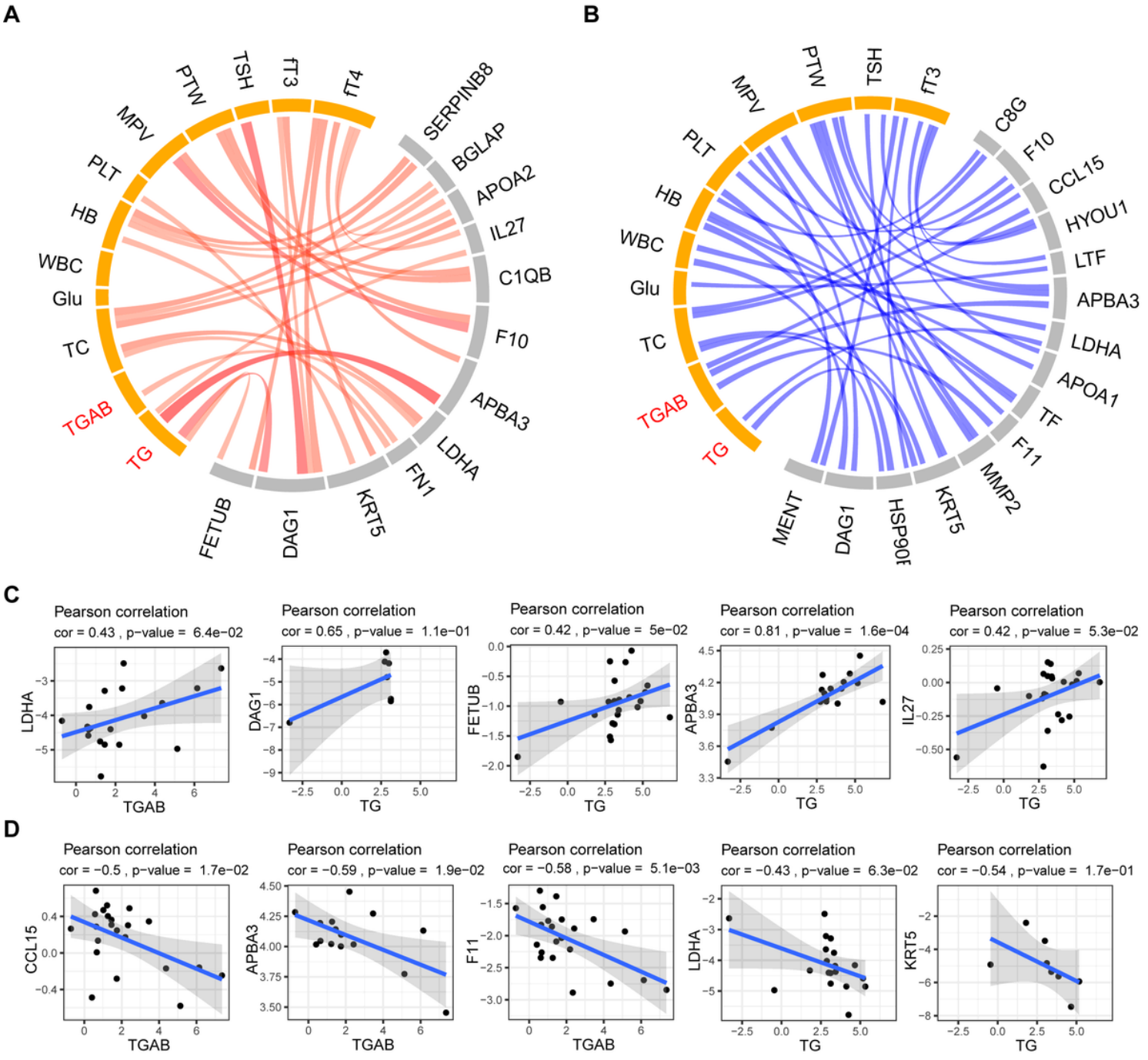

Figure 3

Correlation network of serum proteome and clinical data. (A) Positive and (B) negative correlations between serum proteome and clinical data using circus, respectively. Reprehensive examples for positive (C) and (D) negative correlations.

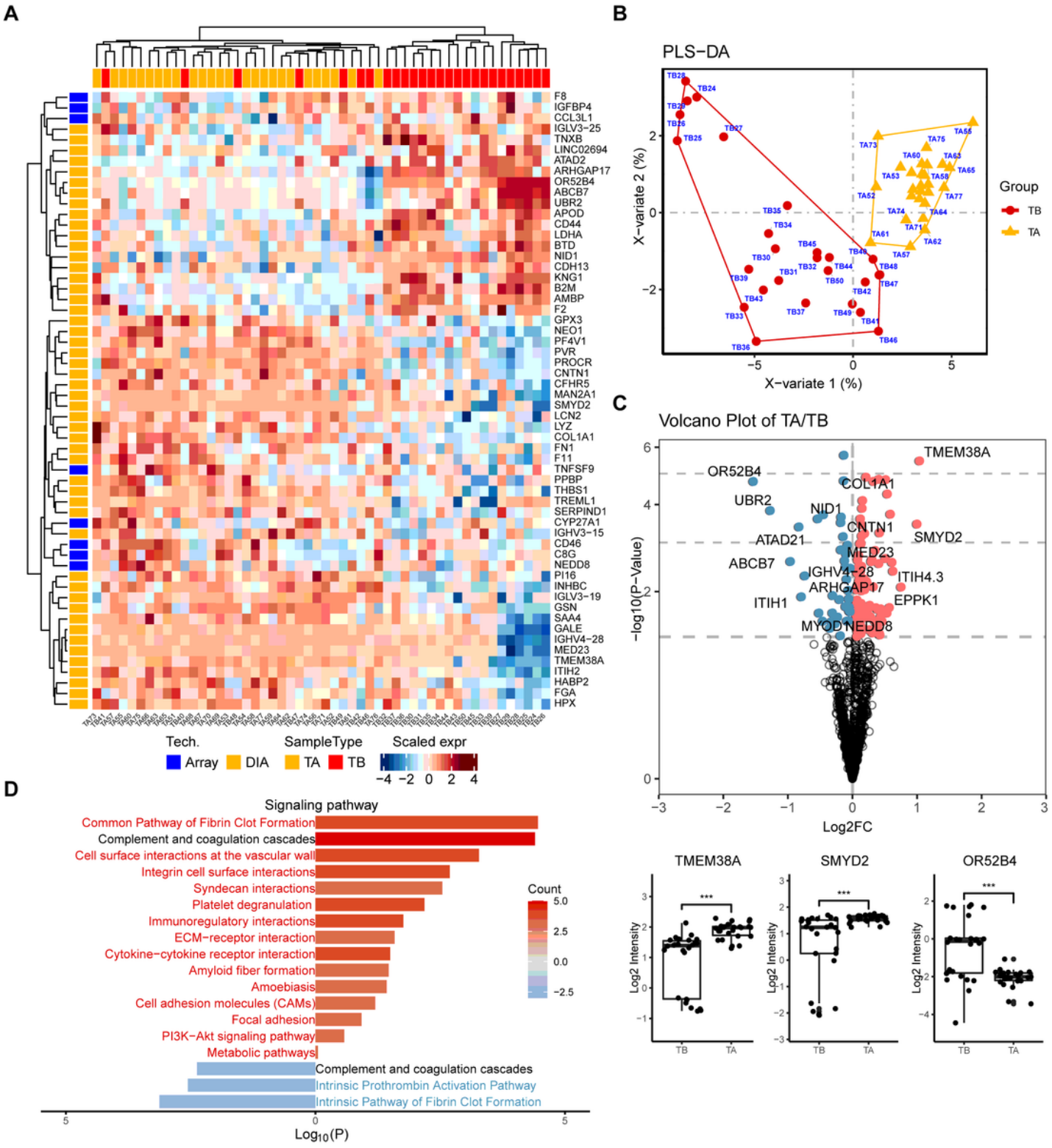

Figure 4

Serum proteome detection consisting of serums before and after surgery for the same pa-tient with papillary thyroid cancer (PTC). (A) Classification of PTC patient before and after sur-gery based on differentially expressed proteins and unbiased clustering analysis. (B) Scores plot for Partial least square-discriminant analysis (PLS-DA). Score plot shows TB in red and TA in blue polygon. (C) Identification of differentiated proteins in serum of PTC patient before and after sur-gery using volcano plot analysis. Box

plot analysis of represented serum proteins. (D) are the comparison of protein classes and signaling pathways for PTC patient before and after surgery.

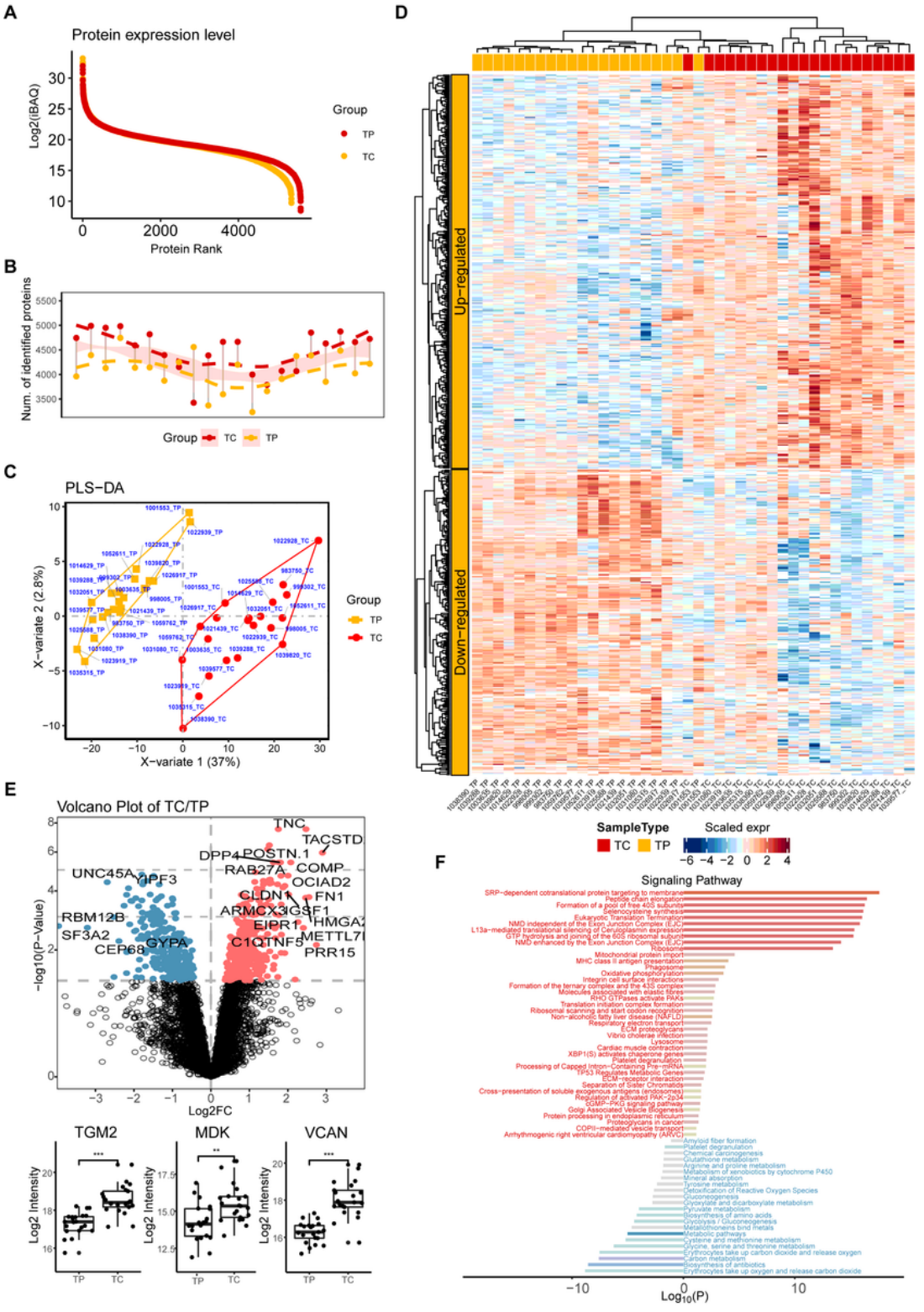

Figure 5

Tissue proteome detection consisting of tumor tissues and their paired non-cancerous adjacent tissues (NATs) for the same patient with papillary thyroid cancer (PTC). (A) The average intensity of the identified

proteins was plotted with rank to illustrate the dynamic range of the tissue proteome. Points in red are the proteins from TC sample and points in orange are the pro-teins form TP. (B) Overview of the protein identifications in TC samples. The pairwise samples are annotated by grey straight lines. The dashed curves fitted by lasso regression show the distribution of protein identifications in TC (red) and TP (orange) samples. The shading that underlies the las-so curves denotes the 95% confidence intervals. (C) Scores plot for Partial least square-discriminant analysis (PLS-DA). Score plot shows TC in red and TP in blue polygon. (D) Classification of tumor tissues and their paired NATs based on differentially expressed proteins and unbiased clustering analysis. (E) Identification of differentiated proteins in tumor tissues and their paired NATs using volcano plot analysis. Box plot analysis of represented proteins. (F) are the comparison of protein classes and signaling pathways for tumor tissues and their paired NATs.

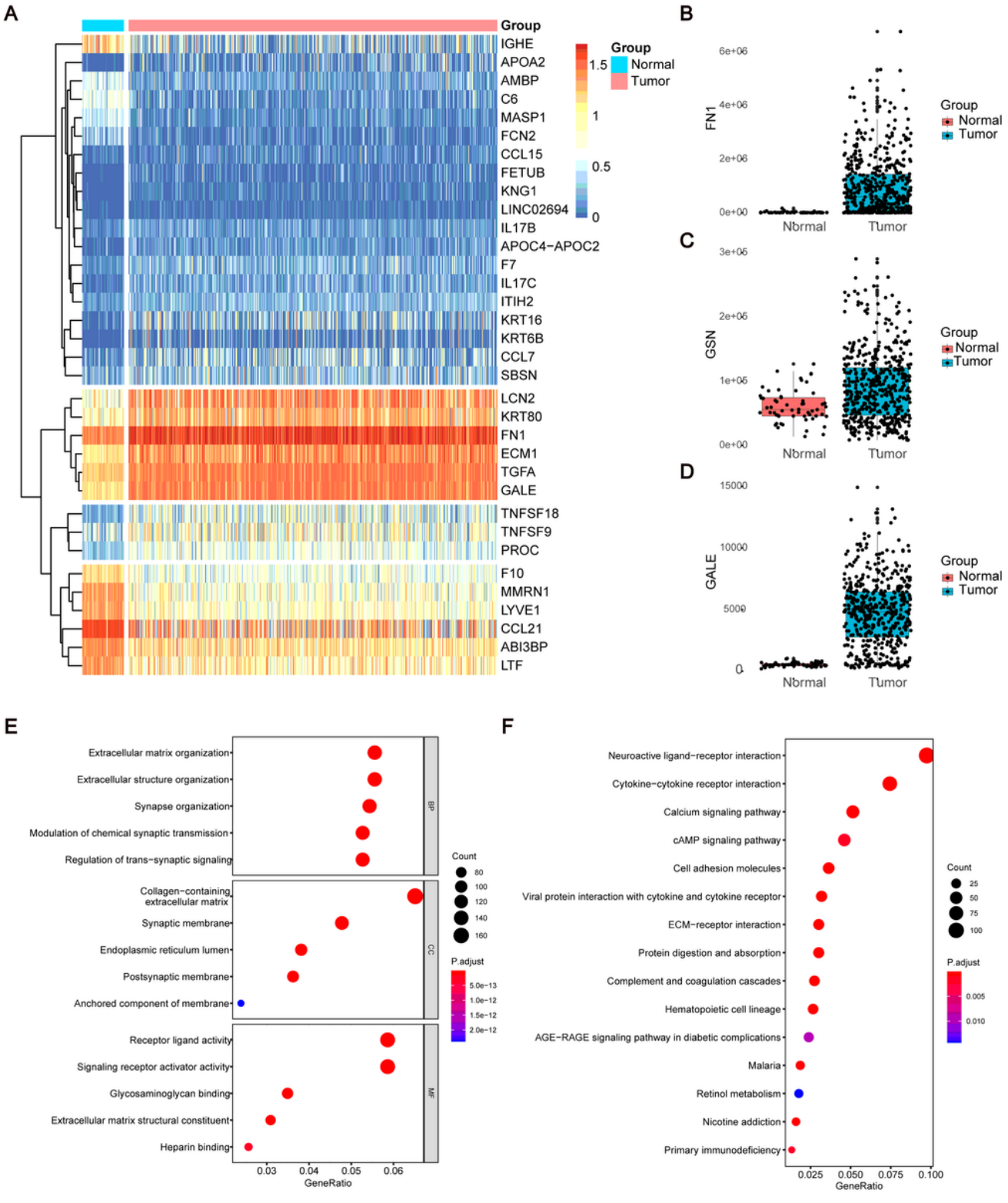

Figure 6

Characterization of the integrated serum and tissue proteomics of patients with papil-lary thyroid cancer. (A) The heatmap of 34 selected genes in TCGA database. (B-D), The boxplots indicate the genes expression levels between Normal and Tumor group. B represents FN1, C rep-resents GSN and D represents GALE, respectively. Red boxplots refer to normal group, while green boxplots are for tumor

group. (E-F) The results of functional enrichment analysis. Size of the dots represent the number of enriched genes, and the color of the dots represent the adjusted P value in GO (E) and KEGG (F) analyses.

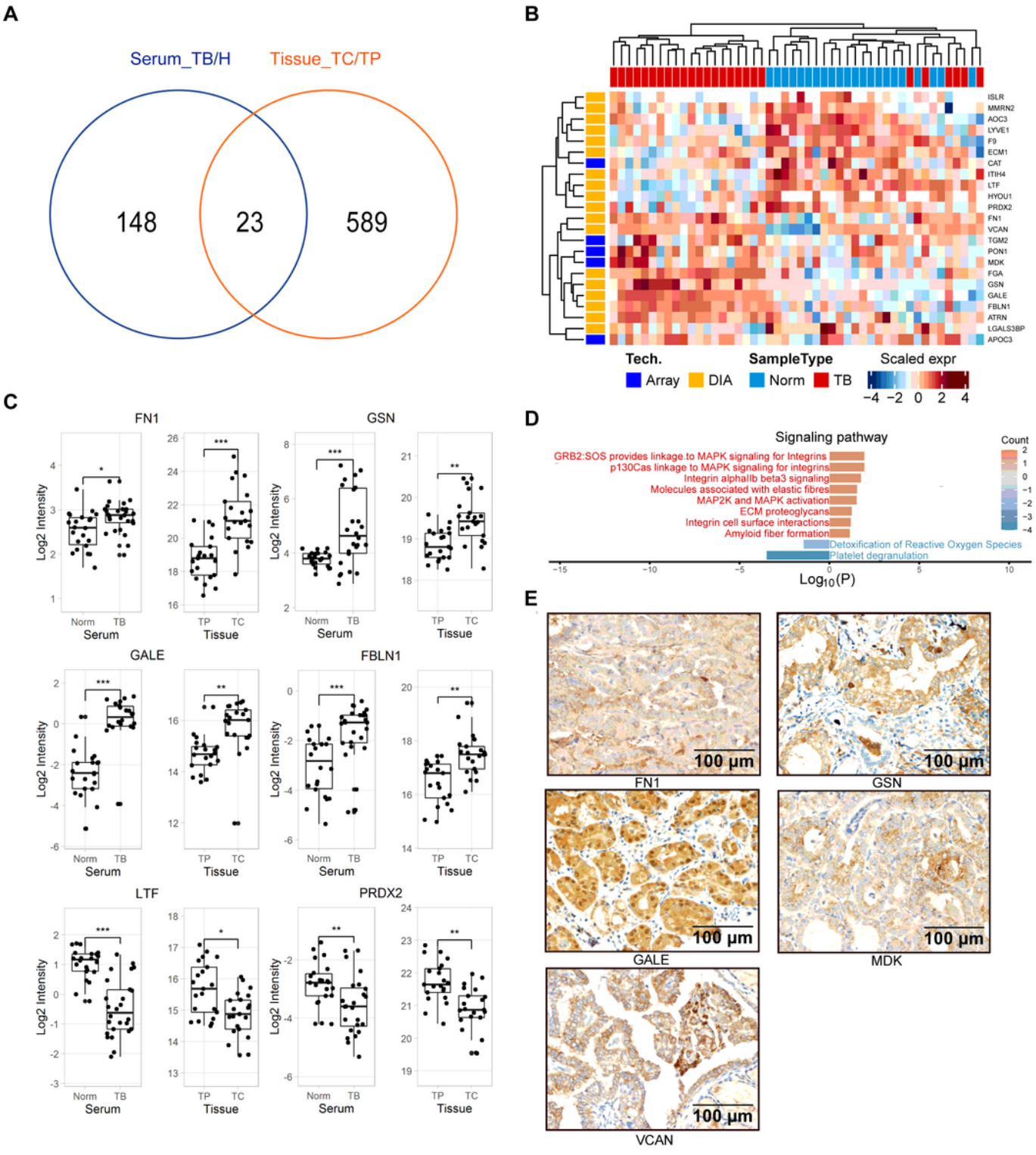

Figure 7

Characterization and validation of the integrated serum and tissue proteomics of pa-tients with papillary thyroid cancer (PTC). (A) the overlapping 23 proteins presented in both se-rum and thyroid tumor tissue

proteomic dataset. (B) Classification of integrated serum and tissue proteomics based on differentially expressed proteins and unbiased clustering analysis. (C) Dif-ferential expressions of represented proteins by DIA-MS and Antibody array. (D) are the compar-ison of protein classes and signaling pathways for 23 overlapped proteins. E, IHC demonstrates represented proteins expressions in PTC tissues. (F-G) Differential serum expressions of FN1 and GSN levels were validated between patients with benign nodules and PTC by Elisa tests in an in-dependent cohort.

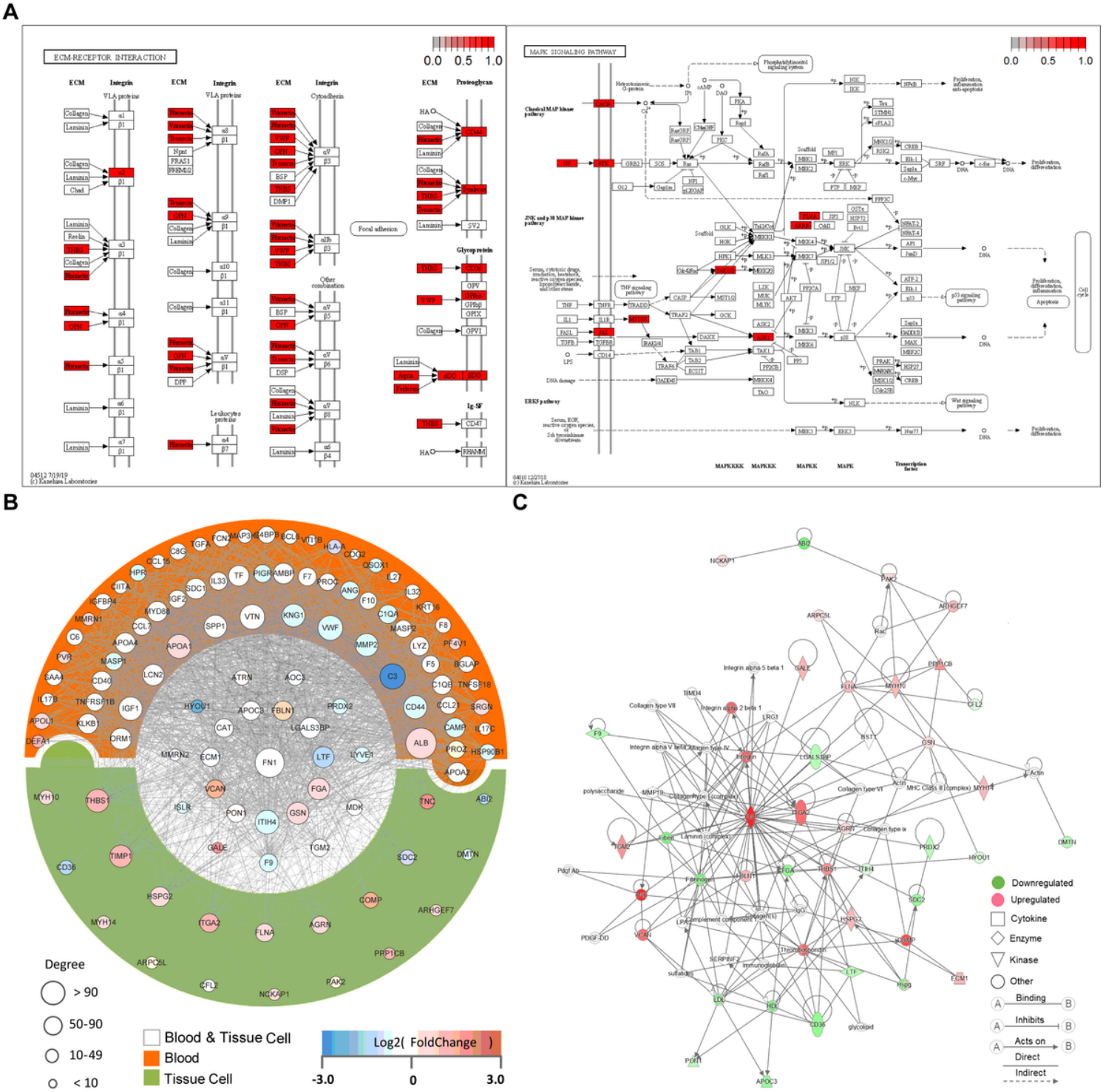

Figure 8

Networking and Cross-talk of the integrated serum and tissue proteomics of patients with papillary thyroid cancer. (A) Extracellular matrix (ECM)-receptor interaction and MAPK pathway. (B) Identified protein interaction between blood and cancer tissue. (C) Ingenuity Path-way Analysis (IPA) Networks of Proteins. (D) Red and green nodes indicate upregulated and downregulated molecules, respectively.

Supplementary Files

This is a list of supplementary files associated with this preprint. Click to download.

- Supplementarymaterial.docx